MRS Advances
https://doi.org/10.1557/s43580-022-00320-4

ORIGINAL PAPER

Evaluation of corrosion behavior of Cu-10Ni alloy in 3 wt% NaCl solution through EIS and ENM methods

Arman Zarebidaki[1] · Seyed Haman Hedaiat Mofidi[1] · Farzaneh Iranmanesh Bahri[1]

Received: 3 June 2022 / Accepted: 13 July 2022

Abstract
The corrosion behavior of Cu-10Ni alloy exposed to 3 wt% NaCl solution was studied via electrochemical impedance spectroscopy (EIS) and electrochemical noise measurement techniques. It was revealed that the charge transfer step, as well as the diffusion through the surface oxide, controls the corrosion. The DC drift (trend) of the electrochemical noise data was removed using discrete wavelet transform. The results obtained through frequency-domain analysis of the data were in good agreement with the EIS results.

Introduction

Excellent biofouling and corrosion resistance and acceptable heat transfer characteristics of copper–nickel (cupronickel) alloy made them well-known structural materials for application in marine and chemical environments [1–3]. The corrosion properties of cupronickel alloys are affected by the Ni content, so increasing the Ni content leads to higher corrosion resistance [4]. In a neutral chloride-containing solution, the corrosion rate is a function of Ni content and the solution chloride ion concentration. With increasing the Ni content up to 65 mass%, the corrosion rate decreases. Furthermore, by increasing the chloride ion concentration up to a specific value, the corrosion rate increases [5]. This behavior is related to chloride ions' adsorption on the surface of Cu_2O film formed during anodic polarization. This phenomenon leads to more cation vacancies, which decreases the corrosion resistance [6]. In Cu–Ni alloy, chloride ions facilitate the formation on of $NiCl_2$, along with $CuCl_2$ and the Ni enrichment of the surface takes place [7]. Different well-defined methods such as EIS, polarization, and weight loss have been used to investigate the corrosion properties of Cu–Ni alloys in different media so far. Electrochemical noise measurement (ENM) is a real in situ, non-destructive, and non-intrusive technique that can be used in corrosion assessment which is not based on the use of external perturbation [8, 9]. In this method, the self-generated potential and/or current fluctuations derived from any type of corrosion are recorded versus time known as electrochemical noise (EN) data [10]. Time-recorded current and voltage fluctuations are considered as non-stationary and non-linear random processes that show time-varying first moments, such as average value and root mean square [11]. This instability may generate a direct current (DC) drift component. Any DC drift will generate new, false frequency components and change the ENM parameters such as current and voltage standard deviations which leads to wrong noise resistance value as well as the wrong slopes of the power spectral density (PSD) plots at low frequencies [12]. Different methods have been introduced for DC trend removal, such as moving average removal, polynomial fitting, and empirical mode decomposition, which among them, DWT is shown to be a reliable method [13]. Considering the lack of reports dealing with the corrosion assessment of Cu–Ni alloys through ENM, it is worth investigating this method for investigating the corrosion behavior of the alloy. In the current study, the corrosion behavior of Cu-10Ni alloy in 3-wt% NaCl solution was investigated using electrochemical impedance spectroscopy (EIS) and ENM methods and the correlation between them was explored. The DWT was used to remove the DC drift of the recorded EN data before analysis. The Spectral noise resistance plot was obtained and compared to the corresponding Bode plot.

✉ Arman Zarebidaki
a.zarebidaki@aut.ac.ir

[1] Corrosion Engineering and Material Protection Group, Amirkabir University of Technology (Tehran Polytechnic), Bandar Abbas Campus, P.O. Box 15875-4413, Tehran, Iran

Published online: 26 July 2022

Materials and methods

Test specimens (1 cm × 1 cm) were cut from an annealed Cu-10Ni (Cu: 89.0 wt%, Ni: 10.8 wt%, Fe: 0.04 wt%) alloy sheet with a thickness of 3 mm. Each specimen was electrically connected and embedded in two-body epoxy resin so that only 1 cm^2 area of each specimen could be exposed to 3-wt% NaCl solution. The test specimens were carefully polished with up to 1500 grit SiC abrasive paper, degreased with acetone, rinsed with distilled water, and dried with air blow. Each specimen was instantly immersed in 250 ml of 3-wt% NaCl solution. EIS test was conducted after 48 h of immersion at the open-circuit potential (OCP), applying a sinusoidal voltage of 5 mV (vs. OCP) amplitude in the frequency range of 10 kHz–0.01 Hz in a standard three-electrode cell using an Autolab/PGSTAT 302 N equipped with frequency response analyzer (FRA) module. A Platinum plate and an Ag/AgCl electrode were used as the counter and the reference electrodes, respectively. The equivalent circuit simulation program (ZView2) was used for data analysis, synthesis of the equivalent electrical circuit (EEC), and fitting of the experimental data.

For the ENM test, electrochemical potential and current fluctuations were simultaneously recorded using a saturated Ag/AgCl reference electrode and two nominally identical Cu-10Ni specimens with 1cm^2 exposed area as working electrodes. The three electrodes were immersed in 3-wt% NaCl solution, and the distance between the reference and the working electrodes was kept 1 cm. The cell was placed in a Faradic cage and the system was warmed up before conducting the test for 20 min. The noise data were recorded for 1024 s at a sampling rate of 4 points/s after 48 h of immersion. Measurement was performed using the EN module of the Autolab/PGSTAT 302 N system. Matlab software was used to analyze the EN data.

Results and discussion

Figure 1 shows the Nyquist plot and the electrical equivalent circuit (EEC) used to fit the EIS results. The Bode modulus plot is shown in Fig. 2b. In the high-frequency region of the bode diagram, the impedance reaches a constant value independent of the frequency which is typical behavior of a resistor and corresponds to the uncompensated or solution resistance (R_s). In the middle-frequency region, a linear relationship is observed between the impedance and the frequency. In the low-frequency region, a constant amplitude is not reached which may be due to the diffusion process. In the EEC, R_s, R_{ct}, and R_{pf} stand for

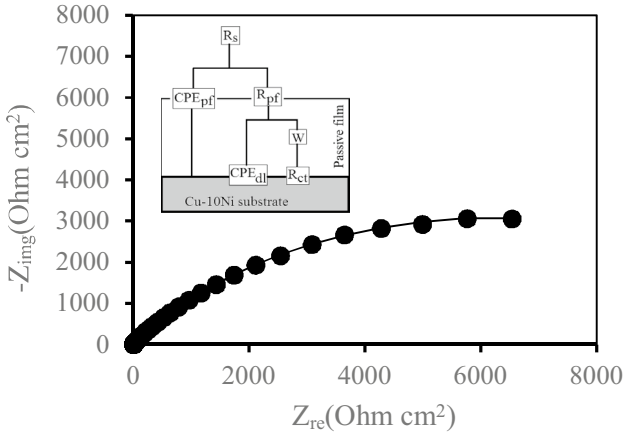

Fig. 1 Nyquist plot and the EEC used to fit the impedance data obtained for Cu-10Ni alloy after 48-h immersion in 3-wt% NaCl

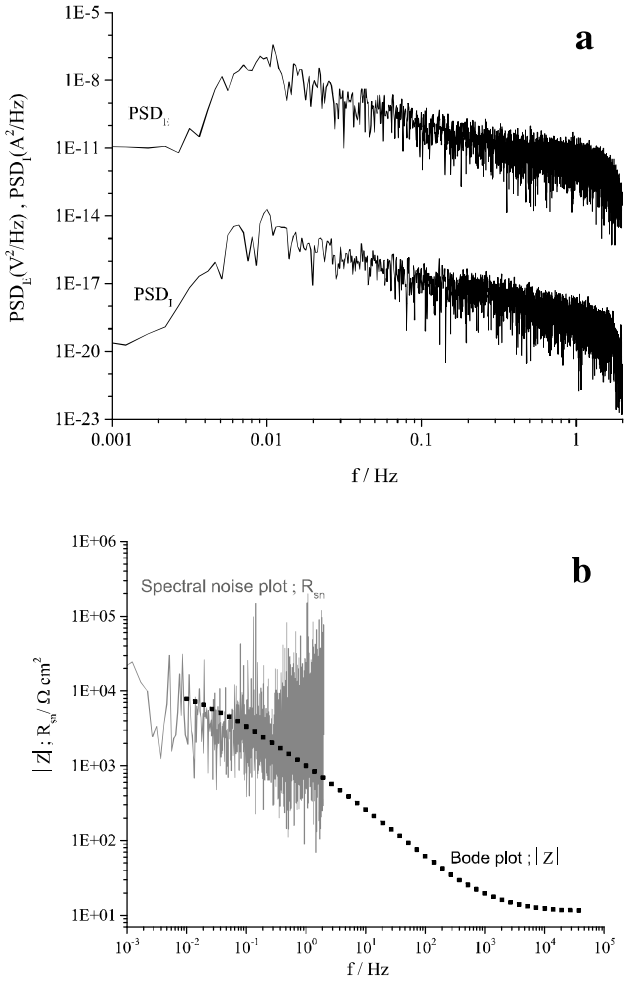

Fig. 2 **a** PSD plots of current and potential and **b** spectral noise and Bode modulus plots obtained for Cu-10Ni alloy after 48-h immersion in 3-wt% NaCl

solution resistance, charge transfer resistance, and passive film resistance, respectively. The polarization resistance Rp value is calculated as $R_p = R_{ct} + R_{pf} + R_w$. CPE stands for the constant phase element and subscripts dl and pf represent double layer and passive film. W is an element for finite layer diffusion thickness [Finite length Warburg (FLW)—short-circuit terminus]. The impedance of FLW is defined as follows [14]:

$$Z_{FLW} = R_w(j\omega\tau)^{-0.5}\tanh(j\omega\tau)^{0.5}, \quad (1)$$

where R_w is the low-frequency limit of Z and $\tau = L^2/D$ (L is the effective diffusion thickness and D is the effective diffusion coefficient). This model implies the presence of an electrode coated by a layer including diffusion. The calculated equivalent circuit parameters are presented in Table 1. For analyzing the EN data the as-received data were first filtered using a low-pass infinite impulse response (IIR) filter with the cutoff frequency of $(2/3)f_{max}$ (Nyquist frequency) [15]. The DC drift (trend) of the filtered data was removed using DWT [16]. The Daubechies wavelet was used for signal decomposition with the J level of 8.

The potential and current mean values (E_{mean} and I_{mean}), potential and current standard deviations ($\sigma[V(t)]$ and $\sigma[I(t)]$), and data skewness and kurtosis are summarized in Table 2. It has been reported that the average kurtosis value below 6 indicates the occurrence of general corrosion [17]. Positive and negative values of potential and current skewness show the positive and negative deviation of the data from a normal distribution. Some researchers reported that skewness and kurtosis are only an indicator of the shape of EN data and cannot imply any mechanistic information [18]. The PSD of potential and current noises are shown in Fig. 2a. Figure 2b shows the spectral noise and Bode plot (obtained from the EIS test). The Spectral noise plot [$R_{sn}(f)$] represents the ratio of the fast Fourier transform (FFT) of potential and current noise and is plotted as a function of frequency (f) in the Bode plot format. Hann window was used for windowing the filtered data [17]. The noise resistance, R_n, is calculated by dividing the standard deviation of potential ($\sigma[V(t)]$) by the standard deviation of current ($\sigma[I(t)]$). For R_n to be equal to R_{ct}, R_n must be independent of frequency, since for a simple R_{ct}-C circuit with a solution resistance of R_s, R_{ct} is defined as [19]

$$R_{ct} = \lim_{f\to 0}(|z(f)|) - R_s. \quad (2)$$

For the EEC model proposed for the current system (Fig. 1)

$$\lim_{f\to 0}(|z(f)|) - R_s = R_p. \quad (3)$$

As aforementioned R_p is the sum of all R-fitted parameters ($R_p = R_{ct} + R_{pf} + R_w$).

The values of S_V, S_I, S_{Rsn}, and R^0_{sn} parameters are summarized in Table 2. S_V and S_I are potential and current PSD slopes and S_{Rsn} is the spectral noise resistance plot slope. The spectral noise resistance (R^0_{sn}) is determined as the average of some data points with the lowest frequencies. For a system with DC limit for $f<f_s$ (f_s is the sampling frequency), R_n will be equal to R_{ct} only if S_V equals S_I [19] and for a capacitive impedance spectrum, when $S_V - S_I = -2$. Theoretical analysis and experimental data have demonstrated that $R_{sn}(f)$ plots and impedance spectra ($\log|z|$ vs. $\log f$) have similar results for the systems with a DC limit [19, 20]. Considering the near-zero value of the S_V-S_I parameter, the $R_{sn}(f)$ plot and impedance spectra show good agreement. Comparing the R^0_{sn} value calculated from EN data (Table 2) and R_p value obtained from EIS measurement (Table 1) reveals that these two parameters have similar values ($R_p = 10$ kΩ.cm^2 and $R^0_{sn} = 9.7$ kΩ.cm^2). It would be noted that R_n and R^0_{sn} are different which can be attributed to the different methods used for

Table 1 Parameters obtained from fitting the EIS data to the proposed EEC

R_s (Ω)	R_{ct} (kΩ cm^2)	CPE_{dl}		CPE_{pf}		R_{pf} (kΩ cm^2)	W		R_p (kΩ cm^2)	χ^2 ($\times 10^{-4}$)
		Q ($\times 10^{-5}$) (S s^n)	n	Q ($\times 10^{-5}$) (S s^n)	n		R (kΩ)	τ (s)		
9.09	2.970	22.63	0.67	17.21	0.77	4.428	2.6	15.67	10	2.7

Table 2 Electrochemical noise parameters of Cu-10Ni alloy in 3-wt% NaCl solution obtained from ENM after 48 h of immersion

Current/A cm^{-2}		Potential/V vs. Ag/AgCl		R_n/kΩ cm^2	R^0_{sn}/kΩ cm^2	S_V	S_I	S_{Rsn}
Mean ($\times 10^{-11}$)	−2.41	Mean ($\times 10^{-7}$)	−4.69					
Skewness	0.1035	Skewness	−0.0822	4.038	9.70	−1.90	−2.02	0.099
Kurtosis	0.7235	Kurtosis	1.0230					
σ ($\times 10^{-9}$)	7.89	σ ($\times 10^{-5}$)	3.1866					

calculating. R^0_{sn} is obtained by extrapolating R_{sn}(f) plot to $f \rightarrow 0$, while R_n is determined at the sampling frequency of 4 Hz [21].

Conclusion

EIS and ENM were used to study the corrosion of Cu-10Ni alloy immersed in 3-wt% NaCl solution. EEC used to fit the EIS data showed that the corrosion of the specimen is controlled by the charge transfer step as well as the diffusion process through the passive film formed after immersion. Statistical analysis of the electrochemical noise (EN) data indicated the occurrence of general corrosion based on the current kurtosis value. The R_{sn} plot obtained from EN data was in good agreement with the Bode plot obtained from the EIS. The R^0_{sn} value was close to the R_p value obtained from EIS. This result reveals that the impedance of the current system can be measured by analyzing the naturally occurring potential and current fluctuations.

Data availability The data that support the findings of this study are available from the corresponding author on request.

Declarations

Conflict of interest The authors declare that they have no known competing financial interests or personal relationships that could have appeared to influence the work reported in this paper.

References

1. K. Chandra, A. Mahanti, A.P. Singh, V. Kain, H.G. Gujar, Eng. Fail. Anal. (2019). https://doi.org/10.1016/j.engfailanal.2019.08.005
2. Z. Dadić, S. Gudić, L. Vrsalović, D. Kvrgić, I. Ivanić, N. Catipovic, Mech. Technol. Struct. Mater. (2019). https://urn.nsk.hr/urn:nbn:hr:115:977236
3. O. Elragei, F. Elshawesh, H.M. Ezuber, Desalin. Water Treat. (2010). https://doi.org/10.5004/dwt.2010.1156
4. D.C. Agarwal, A.M. Bapat, J. Fail. Anal. Prev. (2009). https://doi.org/10.1007/s11668-009-9281-7
5. W.A. Badawy, K.M. Ismail, A.M. Fathi, Electrochim. Acta. (2005). https://doi.org/10.1016/j.electacta.2004.12.030
6. J. Mathiyarasu, N. Palaniswamy, V.S. Muralidharan, J. Chem. Sci. (2001). https://doi.org/10.1007/BF02708553
7. J. Mathiyarasu, N. Palaniswamy, V.S. Muralidharan, Proc. Indian Acad. Sci. (1999). https://doi.org/10.1007/BF02871918
8. F. Mansfeld, J. Electrochem. Soc. (1997). https://doi.org/10.1149/1.1837743
9. S.S. Jamali, D.J. Mills, Prog. Org. Coatings (2016). https://doi.org/10.1016/j.porgcoat.2016.02.016
10. R.A. Cottis, Corrosion (2001). https://doi.org/10.5006/1.3290350
11. D.-H. Xia, Y. Behnamian, Z. Dong, X. Guo, J. Zheng, L. Xu, M. Shahidi, S.M.A. Hosseini, A.H. Jafari, D.-H. Xia, Y. Behnamian, H. Xiao, Russ. J. Electrochem. (2015). https://doi.org/10.1134/S1023193515070071
12. M.K.U. Bertocci, J. Frydman, C. Gabrielli, F. Huet, J. Electrochem. Soc. (1998). https://doi.org/10.1149/1.1838714
13. A.M. Homborg, T. Tinga, E.P.M. van Westing, X. Zhang, G.M. Ferrari, J.H.W. de Wit, J.M.C. Mol, Corrosion (2014). https://doi.org/10.5006/1277
14. M.D. Levi, Z. Lu, D. Aurbach, Solid State Ionics (2001). https://doi.org/10.1016/S0167-2738(01)00819-0
15. R.W. Bosch, R.A. Cottis, K. Csecs, T. Dorsch, L. Dunbar, A. Heyn, F. Huet, O. Hyökyvirta, Z. Kerner, A. Kobzova, J. Macak, R. Novotny, J. Öijerholm, J. Piippo, R. Richner, S. Ritter, J.M. Sánchez-Amaya, A. Somogyi, S. Väisänen, W. Zhang, Electrochim. Acta. (2014). https://doi.org/10.1016/j.electacta.2013.12.093
16. S. Ritter, F. Huet, R.A. Cottis, Werkst. Korros. (2012). https://doi.org/10.1002/maco.201005839
17. C.A. Loto, Int. J. Electrochem. Sci. (2012), Accessed from http://www.electrochemsci.org/list13.htm
18. A.M. Nagiub, Port. Electrochim. Acta. (2017). https://doi.org/10.4152/pea.201704201
19. F. Mansfeld, C.C. Lee, G. Zhang, Electrochim. Acta. (1998). https://doi.org/10.1016/S0013-4686(97)00060-1
20. C.C. Lee, F. Mansfeld, Corros. Sci. (1998). https://doi.org/10.1016/S0010-938X(98)00033-X
21. F. Mansfeld, L.T. Han, C.C. Lee, J. Electrochem. Soc. (1996). https://doi.org/10.1149/1.1837298